Outward stabilization of the S4 segments in domains III and IV enhances lidocaine block of sodium channels

Michael F. Sheets[1] and Dorothy A. Hanck[2]

[1]*The Nora Eccles Harrison Cardiovascular Research & Training Institute and Department of Internal Medicine, University of Utah, Salt Lake City, UT 84112, USA*
[2]*Department of Medicine, University of Chicago, Chicago, IL 60637, USA*

The anti-arrhythmic drug lidocaine has been shown to have a lower affinity for block of voltage-gated sodium channels at hyperpolarized potentials compared to depolarized potentials. Concomitantly, lidocaine reduces maximum gating charge (Q_{max}) by 40% resulting from the complete stabilization of the S4 in domain III in an outward, depolarized position and partial stabilization of the S4 in domain IV in wild-type Na^+ channels ($Na_V1.5$). To investigate whether the pre-positioning of the S4 segments in these two domains in a depolarized conformation increases affinity for lidocaine block, a cysteine residue was substituted for the 3rd outermost charged residue in the S4 of domain III (R3C-DIII) and for the 2nd outermost Arg in S4 of domain IV (R2C-DIV) in $Na_V1.5$. After biotinylation by exposure to extracellular MTSEA-biotin the mutated S4s became stabilized in an outward, depolarized position. For Na^+ channels containing both mutations (R3C-DIII + R2C-DIV) the IC_{50} for rested-state lidocaine block decreased from 194 ± 15 μM in control to 28 ± 2 μM after MTSEA-biotin modification. To determine whether an intact inactivation gate (formed by the linker between domains III and IV) was required for local anaesthetic drugs to modify Na^+ channel gating currents, a Cys was substituted for the Phe in the IFM motif of the inactivation gate (ICM) and then modified by intracellular MTSET (WT-ICM_{MTSET}) before exposure to intracellular QX-222, a quarternary amine. Although WT-ICM_{MTSET} required higher concentrations of drug to block I_{Na} compared to WT, Q_{max} decreased by 35% and the $V_{1/2}$ shifted leftward as previously demonstrated for WT. The effect of stabilization of the S4s in domains III and IV in the absence of an intact inactivation gate on lidocaine block was determined for R3C-DIII + ICM, R2C-DIV + ICM and R3C-DIII + R2C-DIV + ICM, and compared to WT-ICM. IC_{50} values were 1360 ± 430 μM, 890 ± 70 μM, 670 ± 30 μM and 1920 ± 60 μM, respectively. Thermodynamic mutant-cycle analysis was consistent with additive (i.e. independent) contributions from stabilization of the individual S4s in R3C-DIII + ICM and R2C-DIV + ICM. We conclude that the positions of the S4s in domains III and IV are major determinants of the voltage dependence of lidocaine affinity.

(Resubmitted 10 April 2007; accepted 26 April 2007; first published online 17 May 2007)
Corresponding author M. Sheets: CVRTI, Bldg. 500, 95 South 2000 East, University of Utah, Salt Lake City, UT 84112, USA. Email: michael@cvrti.utah.edu

Although local anaesthetics have been in clinical use for more than a century, our understanding of their mechanism of action remains incomplete. When used to relieve peripheral pain their mode of action can be considered as simply blocking the pore of voltage-dependent Na^+ channels referred to as rested state (or tonic) block of ionic current. In contrast, when they are used as anti-arrhythmic agents, the drugs demonstrate a frequency-dependent increase in block termed use-dependent (or state-dependent) block (Strichartz, 1973). The importance of use-dependent block becomes manifest during tachyarrthymias when rapid heart rates increase sodium channel block leading to slower action potential conduction velocities and termination of a reentry-circuit arrhythmia. To account for use-dependent block, it was postulated that the Na^+ channel behaves as a modulated-receptor (Hille, 1977; Hondeghem & Katzung, 1977), where the affinity for drug binding is a function of the channel's kinetic states with a higher affinity for the inactivated state(s) occurring at depolarized potentials compared to the rested state(s) favoured at hyperpolarized potentials. Over

 DOI: 10.1113/jphysiol.2007.134262

the past decade multiple reports (Hanck *et al.* 1994; Balser *et al.* 1996; Hanck *et al.* 2000; Takahashi & Cannon, 2001) have supported the modulated-receptor model, even though the role of drug stabilization of inactivation has been challenged (Vedantham & Cannon, 1999; Hanck *et al.* 2000) and slow-inactivated conformations have also been implicated (Chen *et al.* 2000). Although use-dependent block is readily apparent and therapeutically important, determining the kinetic state(s) of Na^+ channels that contribute(s) to the formation of the higher affinity binding site for local anaesthetic drugs remains controversial (for review see Catterall, 2000; Nau & Wang, 2004), in part because of the difficulty in isolating one kinetic state from another.

Recently, we determined that high affinity lidocaine block was associated with modified movement of the voltage sensors (S4s) in domains III and IV by recording Na^+ channel gating currents (I_g). Lidocaine and lidocaine-like drugs completely inhibited the movement of the S4-DIII by stabilizing it in an outward, depolarized position while the movement of the S4-DIV was only partially inhibited (Sheets & Hanck, 2003). The residual gating charge from the S4-DIV moved with an altered voltage dependence and was responsible for both the observed leftward shift in the $V_{1/2}$ of the Q–V relationship. In contrast, the movements of S4 segments from domains I and II were not modified by lidocaine. The modifications in I_g suggested a model for lidocaine block in which the positions of the voltage sensors in domains III and IV promote the formation of a high affinity lidocaine binding site whereby the bound drug reinforces the modified positions of the two voltage sensors. This interpretation is not dependent on the identification of any specific kinetic state, but rather on the experimentally determined movement of the channel's voltage sensors.

To determine whether the positions of the S4 segments in domains III and IV individually and/or together promote the formation of the high affinity binding site for lidocaine, we created artificial Na^+ channel conformational states in which the S4 segments in domains III and IV were stabilized in an outward, depolarized position independently of membrane potential. The third-outermost basic residue in the S4-DIII (R3C-DIII) and/or the second outermost arginine in the S4-DIV (R2C-DIV) were substituted by a cysteine using site-directed mutagenesis, and stabilization was accomplished by exposure to extracellular MTSEA-biotin. We also investigated whether stabilization of these two S4 segments could increase the affinity for lidocaine block in Na^+ channels without an intact inactivation gate. Previous studies have shown that removal of fast inactivation in Na^+ channels markedly decreased local anaesthetic drug affinity (e.g. Cahalan, 1978; Bennett *et al.* 1995). We found that stabilization of both S4 segments in domains III and IV increased lidocaine affinity in Na^+ channels regardless of whether or not fast inactivation was present suggesting that the outward, depolarized positions of both S4 segments are important factors in promoting the formation of the high affinity binding site of local anaesthetic drugs. The results also suggest that the inactivation gate, while not required for lidocaine binding, contributes to the success of the Na^+ channel in achieving its highest affinity conformation for local anaesthetic drugs.

Methods

Molecular constructs

cDNA for $Na_V1.5$ (hH1a) was kindly provided by H. Hartmann and A. Brown (Hartmann *et al.* 1994). Four-primer PCR (Higuchi *et al.* 1988; Ho *et al.* 1989) was used to substitute a cysteine for the native residue at one or more sites in the channel as follows (using the numbering system of hH1; Makielski *et al.* 2003): (1) the phenylalanine in the IFM motif at amino acid position 1485 (ICM), (2) the third outermost charged residue (an arginine) in DIII at position 1306 (R3C-DIII), and/or (3) the second outermost arginine at position 1626 in DIV (R2C-DIV). These were used to construct WT-ICM, R3C-DIII, R3C-DIII + ICM, R2C-DIV, R2C-DIV + ICM, R3C-DIII + R2C-DIV, and R3C-DIII + R2C-DIV + ICM. The entire inserts containing the mutated sites were confirmed by sequencing. In addition, in all constructs a tyrosine was substituted for the cysteine within the external vestibule of the pore at position 373 (C373Y) to increase the sensitivity to block by tetrodotoxin (TTX) (Chen *et al.* 1996) and to prohibit its reaction with extracellular MTS reagents. For expression in mammalian cells, the cDNAs were subcloned directionally into the mammalian expression vector pRcCMV (Invitrogen, Carlsbad, CA, USA).

Cell preparation

Single tsA201 cells (SV40 transformed HEK293 cells) cells were fused as previously described (Sheets *et al.* 1996) or by the following procedure. tsA201 cells were grown on 100 mm Petri dishes until approximately 95% confluent. Four hours after the addition of fresh standard medium (Dulbecco's modified Eagle's medium (DMEM) from Sigma Corp. supplemented with 10% fetal bovine serum and 1% pencillin–streptomycin), the plate was then washed with medium containing only DMEM. Two millilitres of fusion solution containing 50% polyethylene glycol (M_r 1450, ATCC, Manassas, VA, USA) was added dropwise to the cells before incubating for 10 min at 37°C for 10 min. The fusion solution was then aspirated, 10 ml of standard medium was added, and the cells were placed

back in the incubator at 37°C overnight. The next day the fused tsA201 cells were separated from single cells using a 20 μm mesh filter as previously described (Sheets *et al.* 1996).

In both cases cells were transiently transfected using a calcium phosphate precipitation method (Invitrogen, Carlsbad, CA, USA) either before or after fusion. TTX (600 nM) and/or lidocaine (100 μM) were added to the standard culture medium of cells expressing ICM mutations because anecdotal evidence suggested that expression levels of inactivation-impaired Na^+ channel mutants may be increased. Three to six days after transfection fused cells were detached from culture dishes with trypsin-EDTA solution (Gibco, Grand Island, NY, USA) and studied electrophysiologically.

Recording technique, solutions, experimental protocols and analysis

Recordings were made using a large bore, double-barrelled glass suction pipette for both voltage clamp and internal perfusion as previously described (Sheets *et al.* 1996). I_{Na} and I_g were measured with a virtual ground amplifier (Burr-Brown OPA-101) using a 2.5 MΩ feedback resistor. Voltage protocols were imposed from a 16-bit DA converter (Masscomp 5450, Concurrent Computer, Tinton Falls, NJ, USA or National Instruments, Austin, TX, USA) over a 30/1 voltage divider. Data were filtered by the inherent response of the voltage-clamp circuit (corner frequency near 125 kHz) and recorded with a 16-bit AD converter at 200 kHz. A fraction of the current was fed back to compensate for series resistance. Temperature was controlled using a Sensortek (Physiotemp Instruments, Inc., Clifton, NJ, USA) TS-4 thermoelectric stage mounted beneath the bath chambers and varied less than 0.5°C. Cells were studied at 13°C.

A cell was placed in the aperture of the pipette, and after a high resistance seal had formed the cell membrane inside the pipette was disrupted with a manipulator-controlled platinum wire. Voltage control was assessed by evaluating the time course of the capacitive current and the steepness of the negative slope region of the peak current–voltage relationship as per criteria previously established (Hanck & Sheets, 1992). The holding membrane potential (V_{hp}) was typically set to −150 mV except for cells expressing Na^+ channels with the ICM mutation, where it was −120 mV unless otherwise specified. I_g protocols contained four repetitions at each test voltage that were one-quarter of a 60 Hz cycle out of phase to maximize rejection of this frequency thereby improving the signal to noise ratio.

The control extracellular solution for I_{Na} measurements contained (mM): 15 Na^+ (or 100), 185 TMA^+ (or 100), 2 Ca^{2+}, 200 Mes^- and 10 Hepes (pH 7.2), and the intracellular solution contained 200 TMA^+, 75 F^-, 125 Mes^-, 10 EGTA, and 10 Hepes (pH 7.2). For measurement of I_g the intracellular solution remained unchanged while the extracellular solution had Na^+ replaced with TMA^+ and 1 μM saxitoxin was added (Calbiochem Corp., San Diego, CA, USA). For modification by external *N*-biotinoylaminoethylmethanethiosulphonate (MTSEA-biotin) or by *N*-biotinoylcaproylaminoethyl methanethiosulphonate (MTSEA-biotincap) a 1.0 mM solution was made by initially dissolving the agent in 20 : 1 dimethyl sulfoxide (DMSO) before adding the mixture to 10 ml of extracellular solution (making a 1 : 500 ratio of DMSO to solution). The cell was then perfused with the biotin solution for about 20 min while the membrane potential was stepped from −120 mV to 0 mV for 100 ms at 1 Hz. Control studies on WT-ICM exposed to extracellular MTSEA-biotin showed no effect on I_{Na} or peak current–voltage (I–V) relationships ($n = 2$ cells, data not shown). 2-Trimethylammonium ethylmethanothiosulphonate (MTSET) was dissolved in the perfusate solutions just prior to its use. For intracellular application of MTSET, 2.5 mM was added to the intracellular solution for 8–10 min before switching back to control solutions. While pulsing to −30 mV at 0.5 Hz, the additional slowing of I_{Na} decay in cells expressing the ICM mutation was readily noticeable after 3 min and was typically complete by 10 min. Previous studies have shown that perfusion with $MTSET_i$ under similar conditions did not affect wild-type $Na_V1.5$ (Sheets *et al.* 2000). Cells were first exposed to extracellular MTSEA-biotin before exposure to intracellular MTSET because R2C-DIV is accessible by both extracellular and intracellular sulfhydryl agents (Yang *et al.* 1996). All MTS reagents were from Toronto Chemical Corp., Toronto, Canada. Avidin (Pierce Biotechnology, Rockford, IL, USA) was dissolved in extracellular solutions containing Cl^- because solutions containing MES^- precipitated avidin. For the determination of IC_{50} values, cumulative dose–response curves were constructed by starting with the lowest concentration of lidocaine and incrementing to the next highest concentration. All cells were perfused with lidocaine for at least 3 min before voltage-clamp protocols were started.

Leak resistance was calculated as the reciprocal of the linear conductance (G) between −180 mV and −110 mV, and cell capacitance was measured from the integral of the current responses to voltage steps between −150 mV and −180 mV. For determination of peak I_{Na} voltage relationships, V_{hp} was −150 mV and step potentials were from −130 to 20 mV for 50 ms at 1 Hz. Data were capacity corrected using 4–8 scaled current responses recorded from voltage steps typically between −150 mV and −180 mV. Peak I_{Na} was taken as the mean of four data samples clustered around the maximal value of data digitally filtered at 5 kHz and leak corrected by the amount of the calculated time-independent linear leak. Peak I_{Na}

as a function of potential was fitted with a Boltzmann distribution:

$$I_{Na} = (V_t - V_{rev})G_{max}/(1 + \exp(V_t - V_{1/2}/s)) \quad (1)$$

where I_{Na} is the peak current in response to a step depolarization, and V_t is the test potential. The fitted parameters were $V_{1/2}$, the half-point of the relationship, s, the slope factor in millivolts and V_{rev}, the reversal potential, and $G = I_{Na}/(V_t - V_{rev})$. For comparison between cells, data were normalized to the maximum peak conductance (G_{max}) for each cell.

For I_g measurements the membrane potential was held at −150 mV and stepped to various test potentials for 25 (or 26.5) ms at 1 Hz. All I_g values were leak corrected by the mean of 2–4 ms of data usually beginning 8 ms after the change in test potential and capacity corrected using four to eight scaled current responses to steps between −150 mV and −180 mV taken immediately before and after the test step. To determine time constants of I_g decay, current traces were trimmed until the decay phase was clearly apparent, and then fitted by a sum of up to two exponentials with DISCRETE (Provencher, 1976), a program that provides a modified F statistic in order to evaluate the number of exponential components that best describe the data. Because two exponential fits were better only 28% of the time for R3C-DIII and only 12% of the time for R2C-DIV, single exponential fits were selected for plotting.

Q–V relationships were fitted with a simple Boltzmann distribution:

$$Q = Q_{max}/(1 + \exp(V_t - V_{1/2})/s) \quad (2)$$

where Q is the charge during depolarizing step and V_t is the test potential, and the fitted parameters are Q_{max}, the maximum charge, $V_{1/2}$, the half-point of the relationship, and s, the slope factor in millivolts. Fractional Q was calculated as Q/Q_{max}.

Steady-state voltage-dependent Na^+ channel availability was evaluated from peak I_{Na} in voltage steps to 0 mV after conditioning for 500 ms over a range of potentials. Cycle frequency was 0.5 Hz, and V_{hp} between conditioning steps was −150 mV. Peak I_{Na} as a function of conditioning potential was fitted with a Boltzmann distribution:

$$I_{Na}/I_{max} = (1/(1 + \exp(V_c - V_{1/2}/s))) + I_r \quad (3)$$

where I_{Na} is the peak current after the conditioning pulse, I_{max} is the maximal I_{Na}, V_c is the conditioning potential, I_r is the residual current if I_{Na} did not fully inactivate at the most positive V_c (for channels with the ICM mutation), $V_{1/2}$ is the half-point of the relationship, and s is the slope factor in millivolts.

Single-site binding curves were fitted by:

$$\text{Fractional } G_{max} = 1/(1 + (\text{dose}/IC_{50})) \quad (4)$$

where fractional G_{max} was normalized to G_{max} in control, dose was the concentration of lidocaine, and the IC_{50} was the effective concentration at one-half the reduction in G_{max}.

Interactions between lidocaine and Na^+ channel mutations were calculated according to thermodynamic mutant cycle analysis (Horovitz & Fersht, 1990; Hidalgo & MacKinnon, 1995) where the coupling coefficient, Ω, was calculated by:

$$\Omega = IC_{50(WT-ICM)} \times IC_{50(R2CDIII+R3CDIV+ICM)} / IC_{50(R3CDIII+ICM)} \times IC_{50(R2CDIV+ICM)} \quad (5)$$

where $IC_{50(WT-ICM)}$ is the IC_{50} for block of WT-ICM by lidocaine, etc. Coupling energy was calculated as

$$\text{Coupling energy} = RT \times \ln \Omega \quad (6)$$

where R is the gas constant of 1.98 cal K^{-1} mol^{-1} and T is the absolute temperature.

Data were analysed and graphed on a SUN Sparcstation using SAS (Statistical Analysis System, Cary, NC, USA) or Matlab (The Mathworks, Natick, MA, USA) and Origin (OriginLab Corp., Northhampton, MA, USA). Unless otherwise specified summary statistics are expressed as means ± 1 standard deviation (S.D.). Figures show means ± standard error of the mean (S.E.M.). Student's t test for paired or non-paired data was used to determine statistical significance at the $P < 0.05$ level.

Results

Extracellular MTSEA-biotin stabilized the S4 segments in R3C-DIII and R2C-DIV

We used a variation of the tethered biotin and avidin approach first used with colicin (Qiu *et al.* 1994; Slatin *et al.* 1994), and then in KvAP channels, whereby a site-directed cysteine substitution was made in the S4 segment and biotinylated with a sulfhydryl-reactive agent followed by exposure to avidin (Jiang *et al.* 2003). To confirm that a similar approach could stabilize the S4 of domain III (presumably in an outward, depolarized position), we substituted a cysteine for the third outermost positively charged residue, an arginine (R3C-DIII). We chose this position because it was the most inward (i.e. toward the intracellular space) that could be readily modified by extracellular MTS reagents. Previously, we had shown that R4C-DIII could be modified by intracellular MTSET (Sheets & Hanck, 2003), and subsequent experiments showed it had little or no apparent modification by 2.5 mM extracellular MTSET even after 20 min of exposure (data not shown).

To determine whether R3C-DIII could be stabilized by MTSEA-biotin$_o$ we recorded I_{Na} (Fig. 1) and I_g (Fig. 2) before and after exposure to MTSEA-biotin$_o$. After

control measurements had been obtained the cell was perfused with 1.0 mM MTSEA-biotin$_o$ while stepping to 0 mV for 100 ms from a V_{hp} of −120 mV at 1 Hz. A reduction in peak I_{Na} began almost immediately, and it stabilized by 10–15 min. After peak I_{Na} became stabilized, the V_{hp} was returned to −150 mV, and I_{Na} and I_g measurements were repeated. G_{max}, calculated from peak *I–V* relationships (eqn (1)), decreased by almost 40%. A similar reduction in I_{Na} was apparent in the voltage-dependent Na^+ channel availability relationship suggesting that the S4-DIII participates in closed-state inactivation, although an effect on slow inactivation cannot be ruled out. Furthermore, the large change in the voltage-dependent Na^+ channel availability relationship suggested that the S4-DIII was stabilized in an outward, depolarized position by biotin as opposed to a normal rested, hyperpolarized position because the latter would not be expected to affect the availability relationship.

There was no difference between modification of R3C-DIII by MTSEA-biotin$_o$ compared to MTSEA-biotincap$_o$, a biotin molecule with a linker about 8 Å longer than that for biotin (Jiang *et al.* 2003; Darman *et al.* 2006), and consequently MTSEA-biotin$_o$ was used because it was less expensive. Initially, we also exposed R3C-DIII cells modified with either MTSEA-biotin$_o$ or MTSEA-biotincap$_o$ to extracellular avidin at 40 μg ml^{-1},

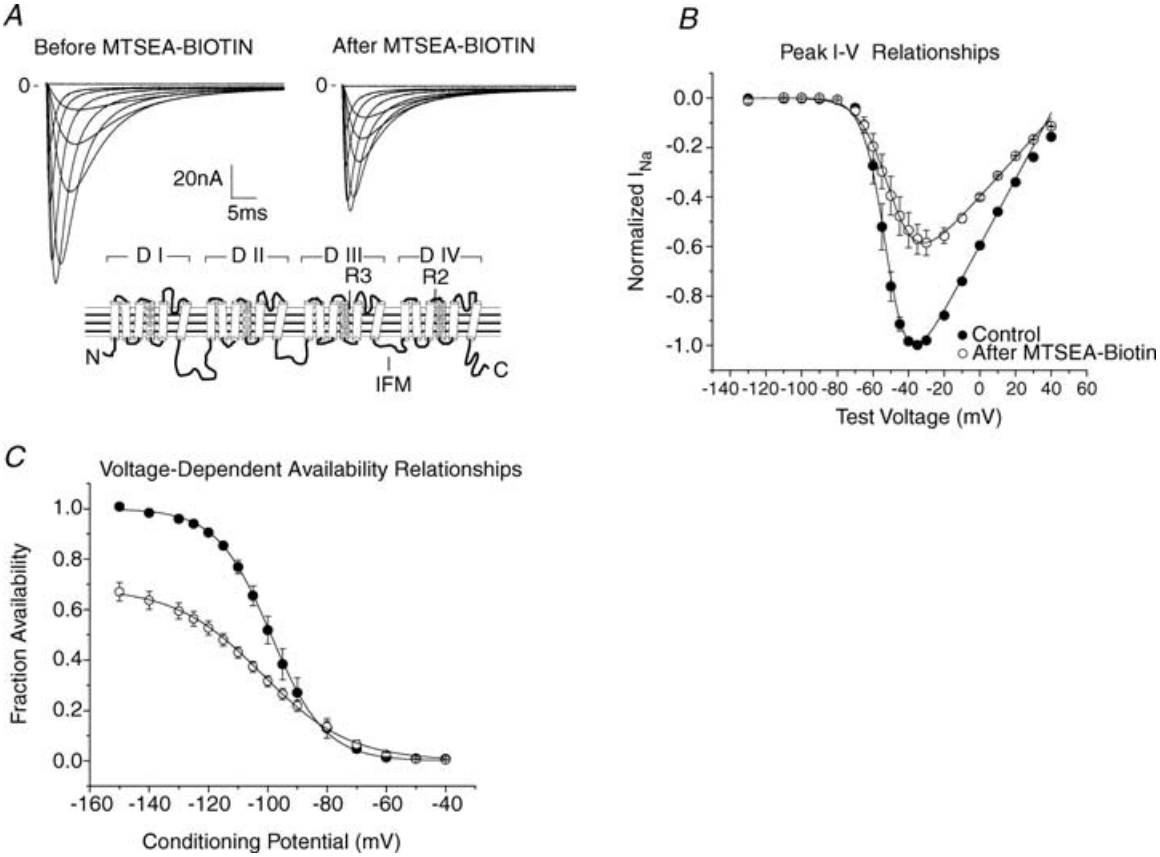

Figure 1. Stabilization of the S4 in R3C-DIII by extracellular MTSEA-biotin
A, family of I_{Na} traces of R3C-DIII in control (left) and after (right) exposure to 1.0 mM MTSEA-biotin$_o$. V_{hp} was −150 mV and step potentials were from −130 to 20 mV for 50 ms. Traces were capacity and leak corrected, and digitally filtered at 5 kHz. The inset shows the predicted secondary structure of the Na^+ channel with R3 in domain III, R2 in domain IV, and the phenylalanine in IFM in the intracellular linker between domains III and IV highlighted. *B*, peak *I–V* relationships ($n = 3$ cells) before (●) and after (○) modification by MTSEA-biotin$_o$ where peak I_{Na} was normalized to the maximum I_{Na} in control. The lines represent the mean of the best fits to eqn (1), and G_{max} in control was used to normalize the values after MTSEA-biotion. The mean parameters showed the G_{max} was decreased to 0.64 ± 0.06, $V_{1/2}$ was unchanged (−52 ± 3 mV and −49 ± 5 mV), and the slope factor decreased from −5.3 ± 0.6 mV to −7.9 ± 0.5 mV. Changes in both the G_{max} and slope factor were statistically significant. *C*, voltage-dependent Na^+ channel availability for 3 cells expressing R3C-DIII in control (●) and after MTSEA-biotin$_o$ (○). The lines represent the mean of the best fits to eqn (3) where I_{Na} was normalized to the maximum value in control for each cell. The normalized maximal I_{Na} decreased to 0.68 ± 0.07, the $V_{1/2}$ shifted to −102 ± 4 mV from −99 ± 4 mV, and the slope factor became more shallow going from 9.2 ± 1.1 mV to 14.7 ± 1.1 mV. The differences in fractional I_{Na} magnitude and slope factor were statistically significant.

but the additional effects on the peak I–V relationship and the voltage-dependent Na^+ channel availability curve were too small (data not shown) to justify using this additional reagent.

Accompanying the decrease in I_{Na}, the Q–V relationship showed a reduction in Q_{max} of 17% while the $V_{1/2}$ and slope factor were not significantly changed (Fig. 2). It is important to note that the individual charged residues in the S4-DIII make different relative contributions to Q_{max}. The S4-DIII as a whole contributes a total of approximately 30% to the Q_{max} in wild-type $Na_V1.5$ with R2 contributing 19%, R3 contributing 10%, and K1 and R4 making little or no contribution (Sheets & Hanck, 2002). Consequently, stabilization of the S4-DIII in R3C-DIII ($Q_{max} = 0.9$ WT) would be predicted to reduce Q_{max} by approximately 21% (calculated from (0.9–0.19)/0.9). The observed 17% reduction in the Q_{max} of R3C-DIII after modification by MTSEA-biotin$_o$ was close to the 21% reduction predicted if the sensor were stabilized in the fully outward position. Single exponential time constants were fitted to I_g decays and are plotted in Fig. 2*B*. Previous studies have shown that the full movement of the S4-DIII in WT human skeletal muscle Na^+ channels ($Na_V1.4$) was completed by depolarization of the membrane potential to −40 mV, and it followed a time course similar to those from the S4s in domains I and II (Cha *et al.* 1999). Consequently, in the unmodified R3C-DIII channel its time course should be slowed compared to those of the S4s in domains I and II because nearly one-third of the gating charge contributed by S4-DIII would have been neutralized by the Cys substitution. However, if the S4-DIII were then stabilized by MTSEA-biotin$_o$, then I_g decay would be expected to become faster because the slow movement by the mutated S4-DIII would be eliminated. This appeared to be the case, and was particularly evident around test potentials of −50 mV.

We used the same approach to stabilize the S4-DIV by exposing R2C-DIV to 1.0 mM MTSEA-biotin$_o$. R2C-DIV was chosen because that arginine has been shown to be externally accessible (Yang *et al.* 1996). It also contributes only ∼9% to Q_{max}, a value similar to that for R3C-DIII (Sheets & Hanck, 2002) while R1 and R3 in domain IV contribute 19% and 4%, respectively, to Q_{max}. Overall, the entire S4-DIV contributes ∼33% to total channel charge (Sheets & Hanck, 2002). Consequently, if the S4-DIV in R2C-DIV ($Q_{max} = 0.91$ WT) were to be fully stabilized, there should be a nearly 25% reduction in Q_{max} $(0.91 - (0.19 + 0.04)/0.91)$. Using the same modification protocol that was described for R3C-DIII, the G_{max} from peak I–V relationship showed a decrease of nearly 40% (Fig. 3) while the voltage-dependent Na^+ channel availability plot showed a prominent leftward shift accompanied by a more shallow slope factor after exposure to MTSEA-biotin$_o$. These data suggest that the S4-DIV may also participate in closed-state inactivation.

After exposure to MTSEA-biotin$_o$, I_g measurements (Fig. 4) showed the Q_{max} was reduced by 25%, the same value predicted if the S4-DIV were stabilized in an outward position. I_g decay time constants became shorter

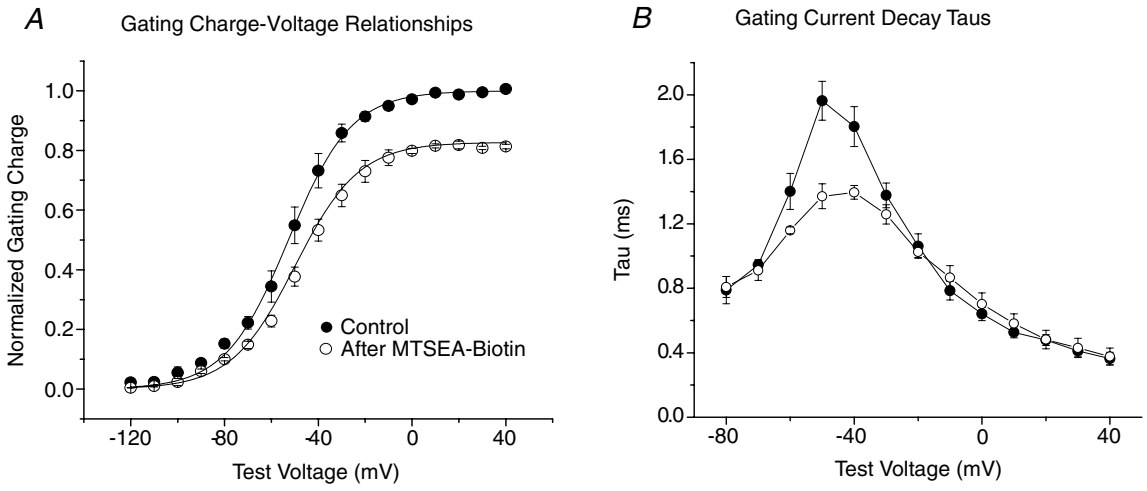

Figure 2. MTSEA-biotin effects on gating charge in R3C-DIII
A, mean Q–V relationships for R3C-DIII ($n = 3$ cells) before (●) and after MTSEA-biotin$_o$ (○) (one cell was modified with MTSEA-biotincap$_o$). Gating charge was normalized to the Q_{max} determined from fits to eqn (2) for each cell in control, and the lines represent the mean of the best fits. After modification by biotin Q_{max} was significantly decreased to 0.83 ± 0.02 while both the change in $V_{1/2}$ (from −54 ± 3 mV in control to −51 ± 3 mV) and the slope factor (from 12.0 ± 1.2 mV in control to 13.1 ± 2.3 mV) were not significantly different. *B*, single exponential fits to the decay of individual I_g traces before and after modification for the same three cells as in *A*. The time constants at −50 mV were significantly different.

after stabilization of the S4-DIV consistent with previous reports that it has the slowest time course compared to the other three S4 segments (Sheets & Hanck, 1995; Sheets *et al.* 1999; Chanda & Bezanilla, 2002). In fact, the changes in time constants of I_g decay after stabilization of the S4-DIV were similar to those previously reported for the decay time constants of I_g in native cardiac Na^+ channels that had been modified by the site-3 toxin Anthopleurin-A, a toxin that has been shown to inhibit movement of the S4-DIV from the rested, hyperpolarized state (Hanck & Sheets, 1995; Sheets & Hanck, 1995). Although we did not perform studies to confirm that the S4-DIV after stabilization by MTSEA-biotin was in an outward, depolarized position, we think such was the case because (1) the Cys substitution was modified by an extracellular applied agent in contrast to one applied intracellularly, (2) inhibiting the movement of the S4-DIV by site-3 toxins has only minimal effects on the Na^+ channel availability curve of cardiac Na^+ channels (Hanck & Sheets, 1995, 2007), in contrast to the large effect of MTSEA-biotin$_o$ on R2C-DIV consistent with stabilization of the S4-DIV in an outward, depolarized position, and (3) I_{Na} continues to demonstrate inactivation during step depolarizations (see Fig. 3*A*) after biotin modification in contrast to the marked prolongation in the decay of I_{Na} after site-3 toxin modification (Hanck & Sheets, 1995). In subsequent studies we stabilized either one or both of the S4s in domains III and IV, and investigated the effects

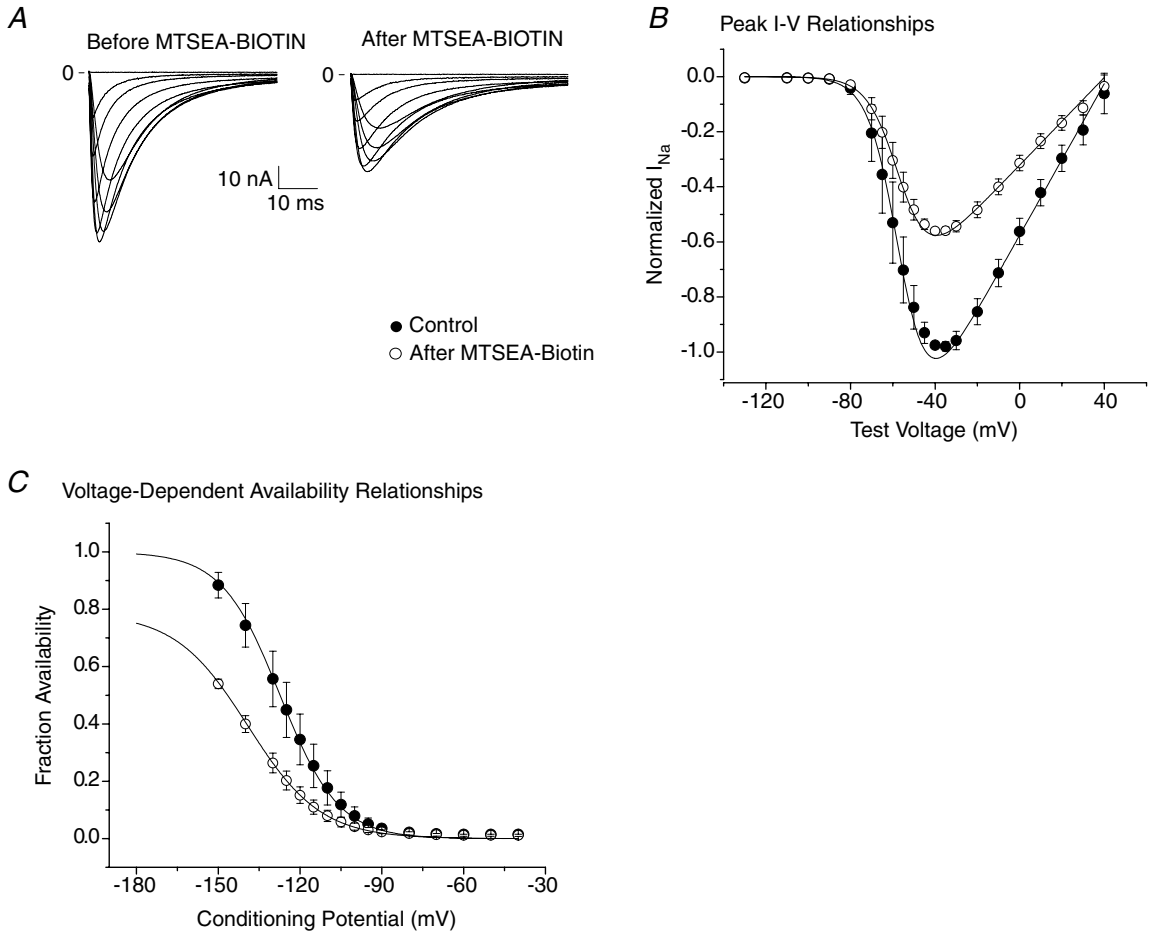

Figure 3. Stabilization of the S4 in R2C-DIV by extracellular MTSEA-biotin
A, family of I_{Na} traces of R2C-DIV in control (left) and after (right) exposure to 1.0 mM MTSEA-biotin$_o$. *B*, peak *I–V* relationships ($n = 3$ cells) before (●) and after (○) modification by MTSEA-biotin$_o$ where peak I_{Na} was normalized to the maximum I_{Na} in control. The lines represent the mean of the best fits to eqn (1), and G_{max} in control was used to normalize the values after MTSEA-biotion. G_{max} was reduced to 0.58 ± 0.03, which was statistically significant. $V_{1/2}$ was -56 ± 7 mV in control and -56 ± 5 mV after modification, and the slope factors were -7.0 ± 0.5 mV in control and -7.3 ± 0.5 mV after modification. For neither was there a significant difference between control and MTSEA-biotin$_o$. *C*, voltage-dependent Na^+ channel availability for three cells expressing R2C-DIV in control (●) and after MTSEA-biotin$_o$ (○). The lines represent the mean of best fits to eqn (3). Normalized maximal I_{Na} decreased to 0.78 ± 0.08, the $V_{1/2}$ shifted leftward from -127 ± 8 mV to -139 ± 4 mV, and the slope factor changed from 10.7 ± 1.0 mV to 13.5 ± 1.9 mV. The differences in all three parameters were statistically significant.

of pre-positioning the voltage sensors on block of I_{Na} by lidocaine.

Stabilization of S4s in both domains III and IV increased block of I_{Na} by lidocaine

Previous studies have shown that lidocaine completely stabilized the S4-DIII in an outward, depolarized position while it only partially stabilized the S4-DIV, altogether producing a reduction in Q_{max} of nearly 40% (Hanck *et al.* 2000; Sheets & Hanck, 2003). If lidocaine block of I_{Na} and its modification of I_g resulted from the same process, i.e. if the translocation of the voltage sensors was associated with the channel's attaining a high affinity conformation, then pre-positioning the S4 segments in domains III and IV would be predicted to make the channel a high affinity lidocaine target. We tested this hypothesis by constructing a Na^+ channel with both the R3C-DIII and R2C-DIV mutation, R3C-DIII + R2C-DIV, and compared lidocaine block of I_{Na} before and after modification with MTSEA-biotin$_o$ (Fig. 5). After exposure to MTSEA-bioin$_o$ peak I_{Na} decreased as expected from the previously demonstrated changes in the voltage-dependent Na^+ channel availability curves of the single mutants, R3C-DIII (see Fig. 1) and R2C-DIV (see Fig. 3). Normalized *G–V* curves were constructed in control, after exposure to increasing concentrations of lidocaine, and after wash for four cells before and after modification by MTSEA-biotin$_o$. The IC_{50} of lidocaine block in the double mutant R3C-DIII + R2C-DIV before stabilization by MTSEA-biotin was $212 \pm 51\ \mu$M, a value similar to that previously reported for first-pulse block of native I_{Na} by lidocaine ($202\ \mu$M) recorded under similar experimental conditions (Hanck *et al.* 2000). After stabilization by MTSEA-biotin$_o$ the affinity for lidocaine block increased to an IC_{50} of $29 \pm 4\ \mu$M, which was comparable to the IC_{50} of $22\ \mu$M found for total block (block that includes first pulse block and use-dependent block) in native I_{Na} during trains of step depolarizations at 10 Hz (Hanck *et al.* 2000). The similarity of the IC_{50s} for R3C-DIII + R2C-DIV before and after stabilization of the S4 segments in domains III and IV compared to first pulse block and total block of native I_{Na} suggest that pre-positioning both S4 segments in domains III and IV by MTSEA-biotin enhances lidocaine block of I_{Na} by reproducing, at least in part, their voltage-dependent positions during lidocaine binding to Na^+ channels.

However, the decrease in the IC_{50} for lidocaine block to $29\ \mu$M in R3C-DIII + R2C-DIV required the stabilization of both S4s and not the stabilization of only one of the S4s. The inset in Fig. 5*D* plots the lidocaine dose–response curves for R3C-DIII and R2C-DIV after each individual mutant channel had been modified by extracellular MTSEA-biotin. Their IC_{50} values were not significantly different ($225 \pm 46\ \mu$M for R3C-DIII and $164 \pm 29\ \mu$M for R2C-DIV); however, the results suggest that stabilization of the S4-DIV may be more important for lidocaine block than that for S4-DIII.

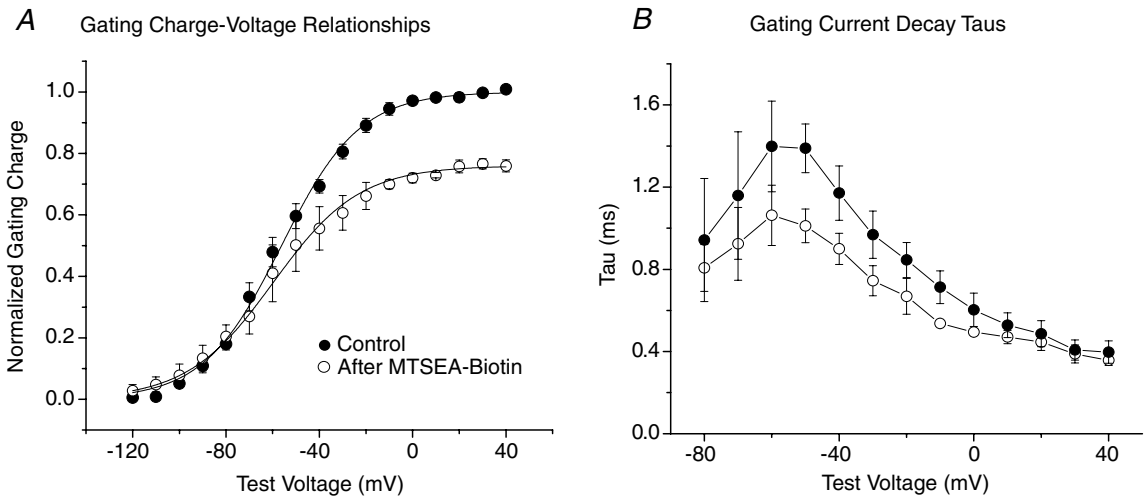

Figure 4. MTSEA-biotin effects on gating charge in R2C-DIV
A, mean *Q–V* relationships for R2C-DIV ($n = 3$ cells) before (●) and after MTSEA-biotin$_o$ (○). The membrane potential was held at −150 mV and stepped to test potentials for 25 ms. Gating charge was normalized to the Q_{max} from the Boltzmann fit (eqn (2)) for each cell in control. After modification Q_{max} was significantly decreased to 0.75 ± 0.03, while both the change in $V_{1/2}$ (from -55 ± 5 mV in control to -60 ± 12 mV) and the slope factor (from 16.6 ± 0.9 mV in control to 18.8 ± 2.3 mV) were not significantly different. *B*, single exponential fits to the decay of individual I_g traces before and after exposure to MTSEA-biotin for the same three cells as in *A*.

QX-222 reduced Q_{max} in Na^+ channels lacking fast inactivation

The removal of fast inactivation in Na^+ channels has been shown to dramatically reduce the affinity of local anaesthetic drugs to block of I_{Na} (Cahalan, 1978; Bennett *et al.* 1995), thereby supporting the hypothesis that local anaesthetic drugs stabilize the inactivated state(s) of the Na^+ channel (Hille, 1977; Hondeghem & Katzung, 1977). However, it is possible that the removal of fast inactivation may only modulate lidocaine's affinity for Na^+ channels without eliminating lidocaine block. If this

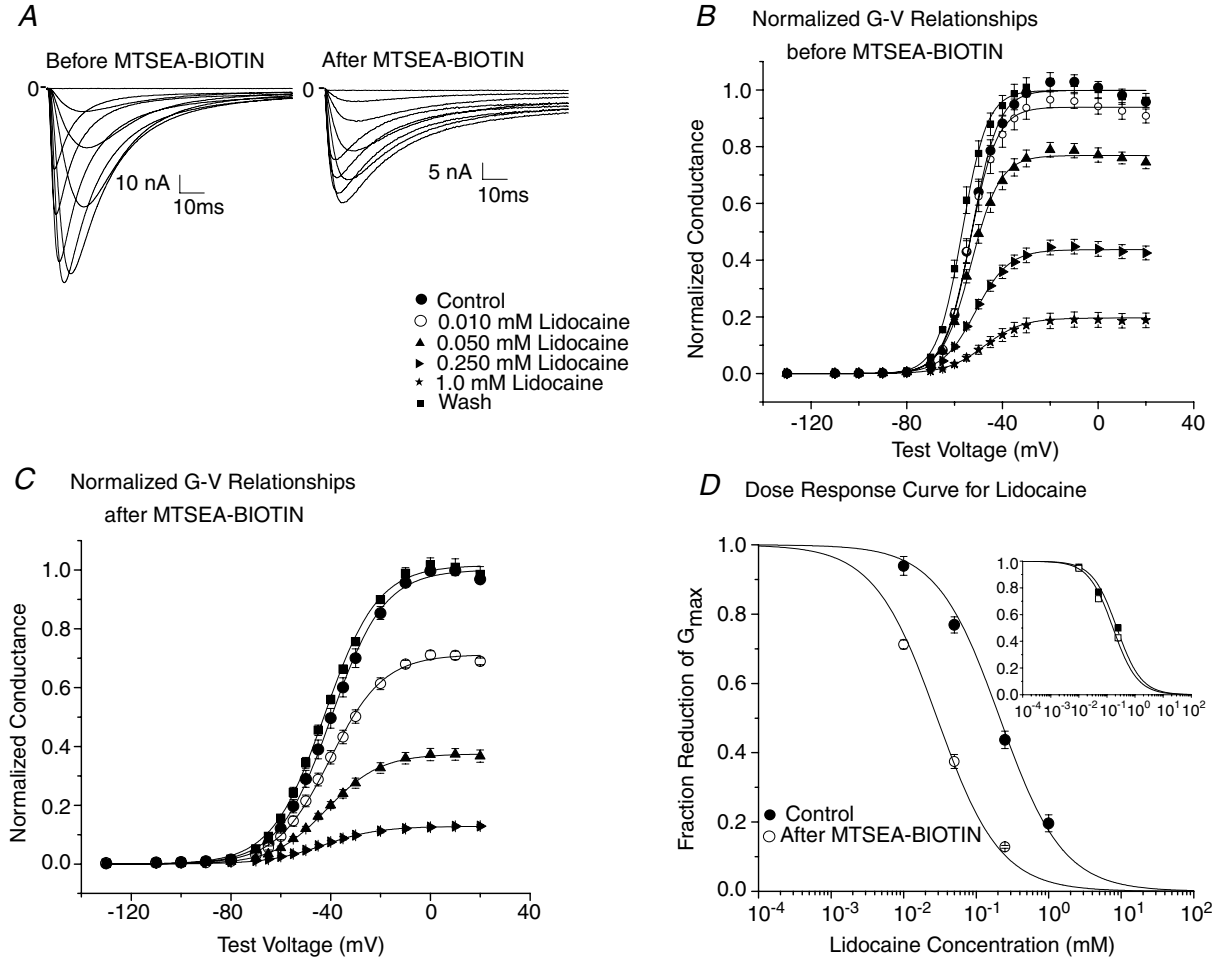

Figure 5. Lidocaine block of MTSEA-biotin modified R3C-DIII + R2C-DIV
A, family of I_{Na} traces of R3C-DIII + R2C-DIV in control (left) and after (right) exposure to 1.0 mM extracellular MTSEA-biotin in 100 mM Na_o. *B*, mean normalized peak *G–V* relationships for four cells expressing R3C-DIII + R2C-DIV in control, in lidocaine and after wash. Cells were exposed to increasing concentrations of extracellular lidocaine, and I_{Na} was recorded during step depolarizations from a V_{hp} of −150 mV to test potentials between −130 mV and 20 mV for 50 ms at 1 Hz following an initial pulse train to 0 mV for 10 ms at 1 Hz for 30 steps. Peak *G–V* relationships were constructed from fits to eqn (1) where the G_{max} in control was used to normalize the measurements in lidocaine and after wash. The lines represent the mean of the best fits to each cell. The key to the symbols shown in *A* applies to *B* and *C*. *C*, mean normalized *G–V* relationships for R3C-DIII + R2C-DIV for four cells after exposure to 1.0 mM MTSEA-$biotin_o$ for nearly 20 min while holding the cell at −120 mV and stepping to 0 mV for 100 ms at 1 Hz. After modification, the V_{hp} was returned to −150 mV before current recordings were obtained. Normalized *G–V* relationships were constructed as above. The lines represent the mean of the best fits. *D*, lidocaine dose–response curve for R3C-DIII + R2C-DIV before and after MTSEA-$biotin_o$. The lines represent the means of four individual cell fits to a single site binding equation (eqn (4)) before (●) and after MTSEA-$biotin_o$ (○) using the normalized G_{max} values for each cell from *B* and *C*. MTSEA-$biotin_o$ increased the sensitivity of R3C-DIII + R2C-DIV to lidocaine block by almost 7-fold where the IC_{50} significantly decreased from 212 ± 51 μM to 29 ± 4 μM. The inset shows the mean lidocaine dose–response curves for R3C-DIII (■) and R2C-DIV (□) both obtained after modification by MTSEA-$biotin_o$. The curves were constructed as described above for R3C-DIII + R2C-DIV. The mean IC_{50} was 225 ± 46 μM for R3C-DIII ($n = 4$ cells), and it was 164 ± 29 μM for R2C-DIV ($n = 4$ cells), which were not statistically different.

were the case, then alteration of the Q–V relationship by local anaesthetic drugs should still occur in Na^+ channels that have impaired fast inactivation, although higher drug concentrations may be required. To determine whether the inactivation gate must be intact for local anaesthetic drugs to modify the Q–V relationship, we investigated $Na_V1.5$ channels without inactivation by substituting a Cys for the Phe in the IFM motif in the domain III–IV linker (WT-ICM) and then modifying it by intracellular MTSET (Vedantham & Cannon, 1998; Sheets *et al.* 2000).

In WT-ICM 2.5 mM MTSET was perfused intracellularly for about 10 min to remove residual I_{Na} decay (Sheets *et al.* 2000; Sheets & Hanck, 2005). After washout of $MTSET_i$ Q–V relationships were obtained in control solutions and after exposure to 20 mM intracellular QX-222 for five cells (Fig. 6*A*). Previous studies in native cardiac Na^+ channels have shown that QX-222_i, a quaternary amine, decreases Q_{max} by ∼40% accompanied by both a hyperpolarizing shift in the $V_{1/2}$ and development of a shallow slope factor (Hanck *et al.* 1994). We chose QX-222_i for these experiments because the very high concentrations of lidocaine that were necessary to fully block channels (> 40 mM) produced a decrease in membrane capacitance presumably though a non-specific action on the lipid membrane. In two cells QX-222_i block was reversed by perfusion with control intracellular solution over ∼20 min. Similar to the effects of QX-222_i on native cardiac Na^+ channels with fast inactivation intact, the quaternary amine decreased Q_{max} by 35%, $V_{1/2}$ was shifted to hyperpolarized potentials, and the slope became more shallow. In addition, I_g relaxations became faster (Fig. 6*B*). Each an effect was similar to that previously reported for native cardiac Na^+ channels (Hanck *et al.* 1994). After washout of QX-222_i the Q–V relationship returned towards control. These results indicate that the presence of an intact fast inactivation gate is not required for local anaesthetic drug modification of Na^+ channel I_g, although the affinity for the drug is much reduced.

Relative contributions of stabilization of R3C-DIII and/or R2C-DIV to lidocaine block of Na^+ channels without an intact fast inactivation gate

Previous recordings of gating charge during recovery from fast inactivation in wild-type Na^+ channels have shown both fast and slow (i.e. immobilized) components (Armstrong & Bezanilla, 1977; Meves & Vogel, 1977; Nonner, 1980; Starkus *et al.* 1981; Greeff *et al.* 1982) with the immobilized component resulting from the slow movement of the S4 segments in both domains III and IV (Cha *et al.* 1999). Subsequently, it was shown that for Na^+ channels with the fast inactivation gate mutated to ICM and modified by $MTSET_i$ the S4-DIV still retained slow kinetics during repolarization. In contrast, the S4-DIII was no longer immobilized, and it moved with a fast time course like that from the S4 segments in domains I and II (Sheets *et al.* 2000; Sheets & Hanck, 2005). Because an intact inactivation gate slows the movement of

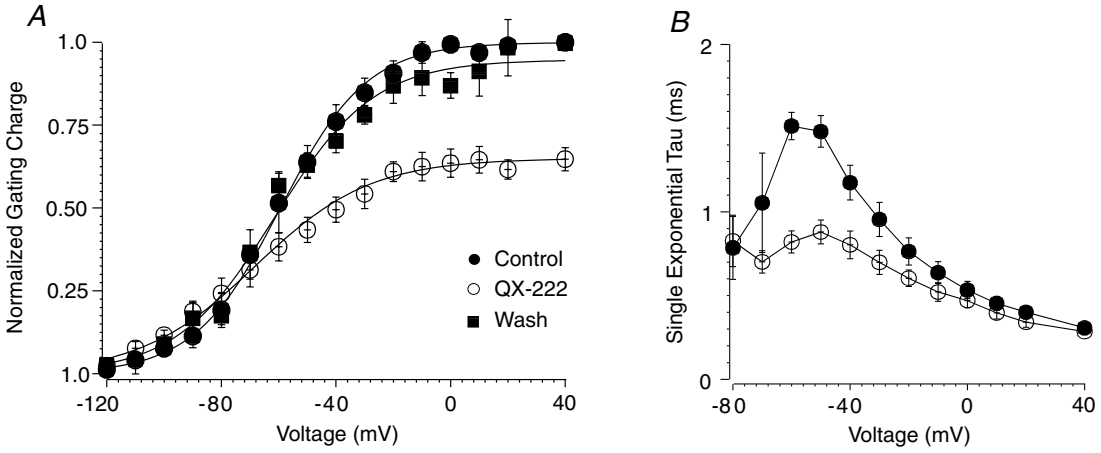

Figure 6. The effects of QX-222 on the Q–V relationship of WT-ICM
A, after perfusion with intracellular MTSET in WT-ICM, Q–V relationships were obtained in five cells before and after the application of 20 mM intracellular QX-222. In two cells Q–V relationships were also obtained after washout of QX-222. Prior to I_g measurements in QX-222, the cells were pulsed to 0 mV for 50 ms at 1 Hz for 10 min to develop greater that 95% block of I_{Na} (data not shown). The membrane potential was held at −150 mV. Gating charge was normalized to the Q_{max} from the Boltzmann fit (eqn (2)) for each cell in control. After exposure to QX-222 Q_{max} was decreased by 35 ± 7% with the $V_{1/2}$ shifting leftward from −60 mV ± 10 mV to −68 ± 11 mV, and a change in the slope factor from −15 ± 0.7 mV to −20 ± 3.4 mV. All three parameters were statistically significant. *B*, single exponential fits to the decay of individual I_g traces before and after exposure to 20 mM QX-222. The time constants at test potentials from −60 to −20 mV were significantly different from each other.

the S4-DIII during repolarization, and because lidocaine stabilizes the S4-DIII in an outward position, one might expect that biotin-stabilization of the S4-DIII would enhance lidocaine block more than stabilization of the S4-DIV in Na^+ channels without intact fast inactivation (ICM_{MTSETi}). To determine the effects of stabilization of the S4 segments in domains III and/or IV on lidocaine affinity we studied R3C-DIII + ICM, R2C-DIV + ICM and R3C-DIII + R2C-DIV + ICM and compared their responses to WT-ICM.

Figure 7 shows the effects of MTSEA-biotin$_o$ and MTSET$_i$ on the modification of the triple mutant,

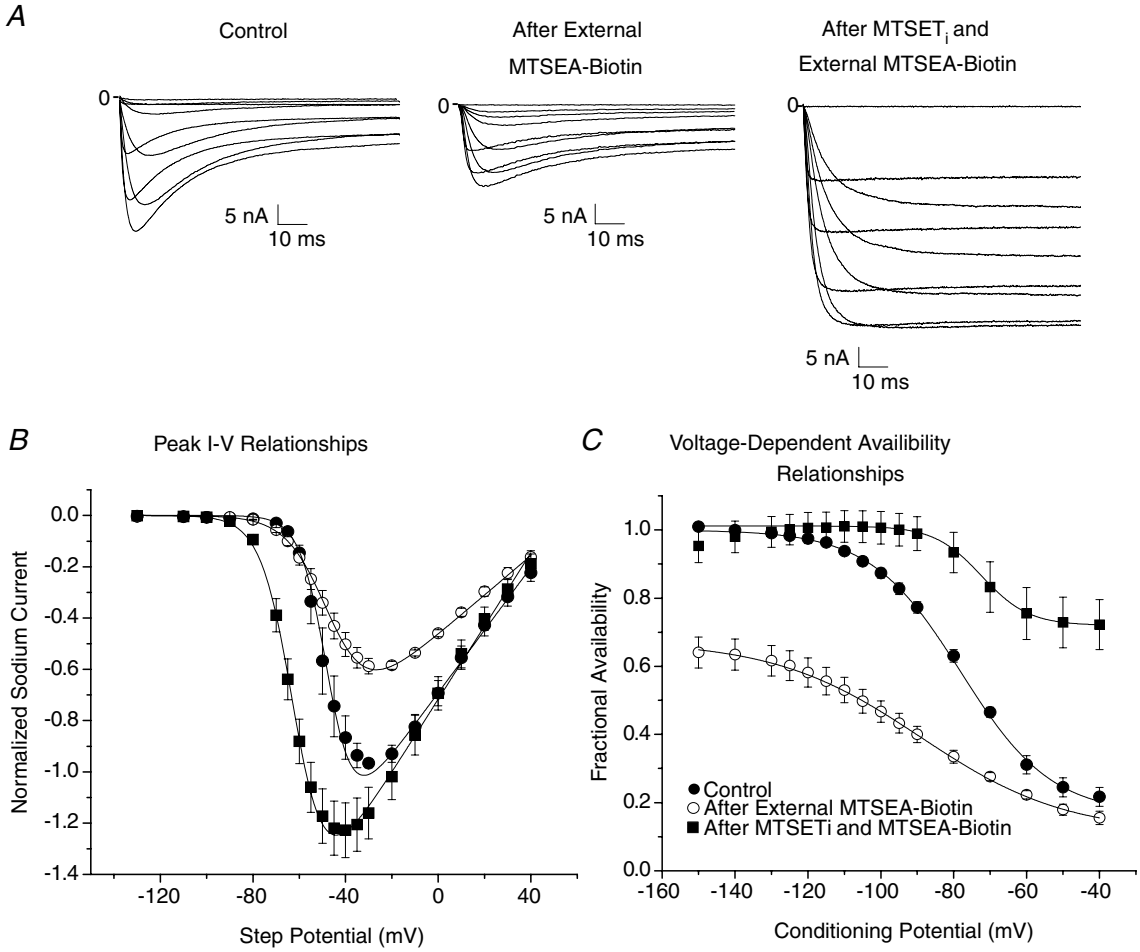

Figure 7. Extracellular MTSEA-biotin and intracellular MTSET modification of R3C-DIII + R2C-DIV + ICM
A, family of I_{Na} traces of R3C-DIII + R2C-DIV + ICM in control solutions (left), after modification by only MTSEA-biotin$_o$ (centre) and after modification by both MTSEA-biotin$_o$ and MTSET$_i$ (right). *B*, peak *I–V* relationships ($n = 4$ cells) in control (●), after modification by only MTSEA-biotin$_o$ (○) and after modification by both MTSEA-biotin$_o$ and MTSET$_i$ (■). Peak I_{Na} was normalized to the maximum I_{Na} in control. The lines represent the mean of the best fits to eqn (1), and G_{max} in control was used to normalize the values after modification. Compared to control values, G_{max} showed a significant decrease to 0.63 ± 0.08 after MTSEA-biotin$_o$, but after both MTSEA-biotin$_o$ and MTSET$_i$ it significantly increased to 1.18 ± 0.10. The $V_{1/2}$ in control was -47 ± 7 mV and was not significantly changed after MTSEA-biotin$_o$ (-46 ± 4 mV) although it was significantly hyperpolarized to -61 ± 3 mV after both agents. The slope factor in control was -5.8 ± 1.4 mV and it became significantly more shallow after MTSEA-biotin$_o$ (-8.9 ± 0.6 mV), and steepened after both agents to -7.1 ± 0.7 mV, which was not statistically different from control. *C*, mean voltage-dependent Na^+ channel availability relationships for the same four cells expressing R3C-DIII + R2C-DIV + ICM in control (●) and after only MTSEA-biotin$_o$ (○), and after both MTSEA-biotin$_o$ and MTSET$_i$ (■). The lines represent the mean of the best fits to a Boltzmann relationship (see eqn (3)) across all conditioning potentials except the range was restricted between -120 mV and -40 mV in the cells after both MTSEA-biotin$_o$ and MTSET$_i$. The normalized maximal I_{Na} was significantly decreased to 0.67 ± 0.04 after modification by only MTSEA-biotin$_o$ and then returned back to the control value (1.01 ± 0.04) after fast inactivation had been removed by MTSET$_i$. The fraction of non-inactivating I_{Na} after both agents was 0.72 ± 0.07. $V_{1/2}$ in control was shifted significantly leftward from -78 ± 2 mV to -89 ± 3 mV after MTSEA-biotin$_o$, and then shifted rightward to -72 ± 2 mV after MTSET$_i$ (not significantly different compared to control). The slope factor in control (12.4 ± 0.6 mV) was significantly different from that after MTSEA-biotin$_o$ (20.0 ± 1.2 mV) and after both agents (6.5 ± 0.3 mV).

R3C-DIII + R2C-DIV + ICM. Because R2C-DIV is accessible by both extracellular and intracellular sulfhydryl agents (Yang *et al.* 1996), in these experiments the cysteines on the S4 segments were first exposed to MTSEA-biotin$_o$ before the cell was perfused with intracellular MTSET. Figure 7*A* shows I_{Na} in response to step depolarizations in control solutions, after modification by MTSEA-biotin$_o$, and after both MTSEA-biotin$_o$ and MTSET$_i$. Extracellular MTSEA-biotin, by itself, caused a decrease in peak I_{Na} (Fig. 7*B*) secondary to the large change in the voltage-dependent Na^+ channel availability curve (Fig. 7*C*) similar to that for both R3C-DIII (Fig. 1) and R2C-DIV (Fig. 3). After removal of the residual I_{Na} inactivation by intracellular MTSET G_{max} returned to its previous value as the steady-state availability relationship shifted rightward (Fig. 7*C*). Because the maximum Na^+ channel availability occurred at conditioning potentials near −120 mV in R3C-DIII + R2C-DIV + ICM after modification by both agents, the V_{hp} was set to this value for all subsequent studies on lidocaine block of Na^+ channels with ICM mutations.

Lidocaine dose–response curves were generated for R3C-DIII + R2C-DIV + ICM, R3C-DIII + ICM, R2C-DIV + ICM (all after modification by both MTSEA-biotin$_o$ and MTSET$_i$) and compared to WT-ICM after MTSET$_i$ by constructing peak *G*–*V* relationships in control, for increasing concentrations of lidocaine, and after wash. Figure 8 shows the mean results for three to five cells with each mutation. The values for G_{max} were fitted with a single-site binding relationship (eqn (4)) to determine the IC_{50} for each of the four mutant channels. As expected for Na^+ channels with a modified fast inactivation gate, the IC_{50} for WT-ICM was increased (1970 ± 60 μM). After stabilization of both S4s in R3C-DIII + R2C-DIV + ICM the IC_{50} decreased significantly to 670 ± 70 μM. When only one of the two S4 segments was stabilized, the IC_{50} values were between those for WT-ICM and R3C-DIII + R2C-DIV + ICM. However, in contrast to the expectation that stabilization of the S4-DIII would increase lidocaine block more than that for stabilization of the S4-DIV, R3C-DIII had a lower affinity for lidocaine than R2C-DIV (1440 ± 310 μM *versus* 890 ± 150 μM).

To determine whether the changes in the IC_{50} of the S4 mutations were additive (i.e. independent), we applied the technique of thermodynamic mutant-cycle analysis to lidocaine block of the four ICM mutations (Horovitz & Fersht, 1990; Hidalgo & MacKinnon, 1995). If stabilization of the S4 segments in domains III and IV have independent effects then the coupling coefficient, Ω, given by eqn (5) will be unity, and the coupling energy (eqn (6)) will equal zero. However, if the stabilization of one S4 segment were to help stabilize the other S4 segment then the coupling coefficient, Ω, will deviate from unity. Application of thermodynamic mutant-cycle analysis to lidocaine block of the four ICM mutations gives an Ω almost equal to 1 (1.03) suggesting that the increased affinity for lidocaine block following stabilization of both S4 segments is simply the sum of the increased affinity resulting from the stabilization of each individual S4 (Fig. 9*B*).

Discussion

To determine whether pre-positioning the S4 segments in domains III and IV can affect the affinity of lidocaine for block of Na^+ channels we stabilized the S4s in either R3C-DIII and/or R2C-DIV by extracellular MTSEA-biotin before and after exposure to lidocaine. These experiments had three major findings. (1) Pre-positioning the S4s from domains III and IV (presumably in outward, depolarized positions) in Na^+ channels with intact fast inactivation produced a high affinity binding site equivalent to that achieved in WT channels after high frequency depolarizing pulse trains. (2) An intact fast inactivation gate is not required for local anaesthetic drugs to modify Na^+ channel gating currents similar to their effects on WT channels (Hanck *et al.* 1994, 2000), although removal of fast inactivation markedly reduces the channel's affinity for lidocaine (Cahalan, 1978; Bennett *et al.* 1995). (3) When the fast inactivation gate was disrupted in ICM mutant channels, pre-positioning of both S4 segments in domains III and IV also increased lidocaine's blocking affinity consistent with independent (i.e. additive) effects from each of the two stabilized S4 segments.

It is important to note that Na^+ channels with stabilization of the S4s in domains III and/or IV were not intended to simulate a native kinetic state of a wild-type Na^+ channel, but to determine whether or not pre-positioning those S4 segments could modulate lidocaine block. Consequently, these studies do not answer the question as to which state of the WT channel has the highest lidocaine affinity other than to note that it is likely to be a kinetic state in which both the S4 segments in domains III and IV are in an outward, depolarized position. It is easy to speculate that such a position of the S4 segments may help contribute to use-dependent block of I_{Na} by local anaesthetic drugs.

Pre-positioning voltage sensors with the fast inactivation gate intact

We used a variation of the tethered biotin and avidin approach (Slatin *et al.* 1994) to stabilize the S4 segments in domains III and IV. The reductions in gating charge, 17% for S4-DIII and 25% for S4-DIV, were consistent with the predictions of charge reduction based upon the reported contribution of each voltage sensor to total gating charge (Sheets *et al.* 1999; Sheets & Hanck, 2002). However, unlike KvAP channels (Jiang *et al.* 2003), we found that biotin by

itself was sufficient to stabilize the S4 segments without the need to expose the biotinylated S4 to avidin. This may be a consequence of a difference between Na^+ channels and KvAP channels, or it may be because the arginine residues we selected for cysteine substitution were located in a 'deeper' physical position. Also, we did not observe much of a difference between modification with either MTSEA-biotin or MTSEA-biotincap.

Interestingly, stabilization of the S4 in R3C-DIII dramatically affected voltage-dependent Na^+ channel availability, but had minimal effects on the peak *I–V* relationship except for an obvious decrease in G_{max} (see Fig. 1). The lack of a large effect on channel activation was surprising because the S4 segments from domains I, II and III all appear to move before channel opening (Chanda & Bezanilla, 2002). The large change in the Na^+

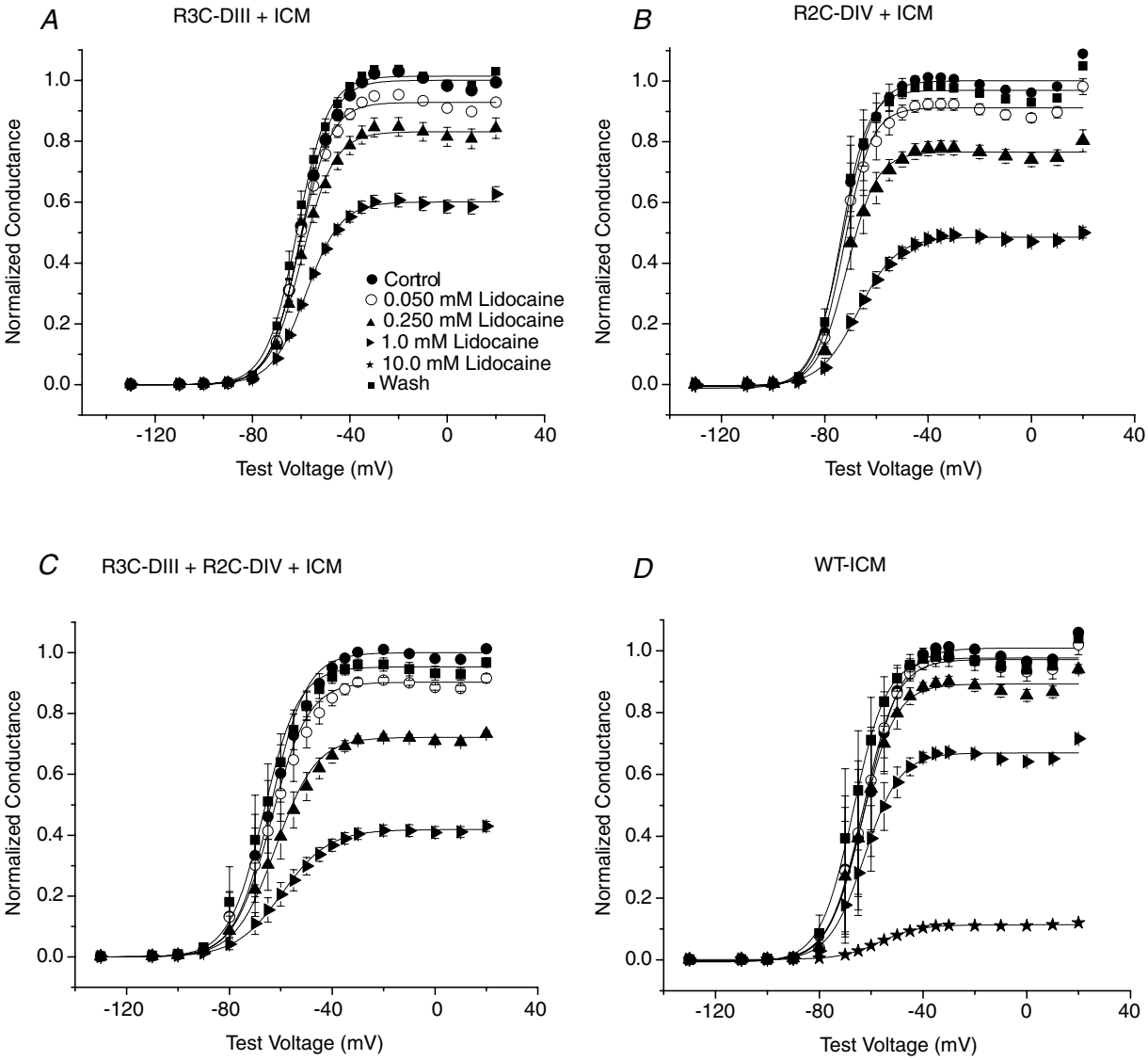

Figure 8. Peak *G–V* relationships before and after lidocaine block in MTSEA-biotin stabilized S4 mutant Na^+ channels with a modified fast inactivation gate (ICM_{MTSET})
R3C-DIII + ICM (*A*), R3C-DIV + ICM (*B*), and R3C-DIII + R2C-DIV + ICM (*C*) were first modified by extracellular MTSEA-biotin before exposure to intracellular MTSET as described in Methods. *D*, the peak *G–V* relationships for WT-ICM after $MTSET_i$. For each mutation and at each concentration of lidocaine the means are from three to five cells (except there is only one WT-ICM cell at a lidocaine concentration of 10 mM). Peak *G–V* relationships were constructed from fits to eqn (1) where the G_{max} in control was used to normalize the measurements in lidocaine and after wash. Cells in control (●) were exposed to increasing concentrations of extracellular lidocaine (0.050 mM (○), 0.250 mM (▲),1.0 mM (▶), 10.0 mM (⋆)) before wash (■), and I_{Na} was recorded during step depolarizations from a V_{hp} of −120 mV. The key to the symbols shown in *A* applies to all four panels. The largest fraction of cumulative block in lidocaine that occurred during any of the above voltage clamp protocols was less than 4% in all of the channel mutations.

channel availability relationship with its more shallow slope factor is consistent with an increase in closed-state inactivation; however, an effect on slow inactivation could not be ruled out. Stabilization of the S4 in R2C-DIV also had similar effects on voltage-dependent Na^+ channel availability accompanied by minimal effects on the peak *I–V* relationship except for an accompanying reduction in G_{max} (Fig. 2). This, however, was less surprising because the S4-DIV has been previously shown to have a unique role in coupling activation to inactivation (Sheets & Hanck, 1995; Yang & Horn, 1995; Sheets *et al.* 1999; Chanda & Bezanilla, 2002). The fact that channel activation was relatively unaffected when both S4 segments in domains III and IV were stabilized by MTSEA-biotin suggests that the S6 segments in domains I and II may contribute the most to opening of the activation gate.

The roles of the S4 segments in domains III and IV and fast inactivation to block of I_{Na} by lidocaine

With fast inactivation intact, pre-positioning both S4s in R3C-DIII + R2C-DIV by MTSEA-biotin produced high affinity lidocaine block with an IC_{50} of 28 μM, a concentration comparable to that previously reported (IC_{50} of 22 μM) for lidocaine block during a fast pulse train (10 Hz) in native cardiac Na^+ channels (Hanck *et al.* 2000). Before pre-positioning the voltage sensors in R3C-DIII + R2C-DIV the IC_{50} for lidocaine was 194 μM, a concentration that was also similar to that for native Na^+ channels at rest (202 μM; Hanck *et al.* 2000) suggesting that the neutralization of the two arginine residues in R3C-DIII + R2C-DIV did not prevent the channel from achieving a conformation similar to that for WT channels (i.e. a 'rested state' conformation).

When the fast inactivation gate was disrupted in WT-ICM by $MTSET_i$ the IC_{50} at the holding potential increased 10-fold (from 194 μM to 1970 μM). After stabilization of both S4s in R3C-DIII + R2C-DIV + ICM the IC_{50} decreased to 670 μM. This higher affinity could be accounted for quantitatively by adding the contributions from the stabilization of each the individual S4s in the two domains (Fig. 9*B*) with the stabilization of the S4-DIV making a larger contribution than the S4-DIII. This result was somewhat surprising given that, with respect to the effects on gating charge, lidocaine completely inhibits movement of S4-DIII while only partially inhibiting movement of the S4-DIV. Consequently, these results suggest the contribution to lidocaine block by pre-positioning the S4-DIV is as important or possibly more important than that for the S4-DIII. It should

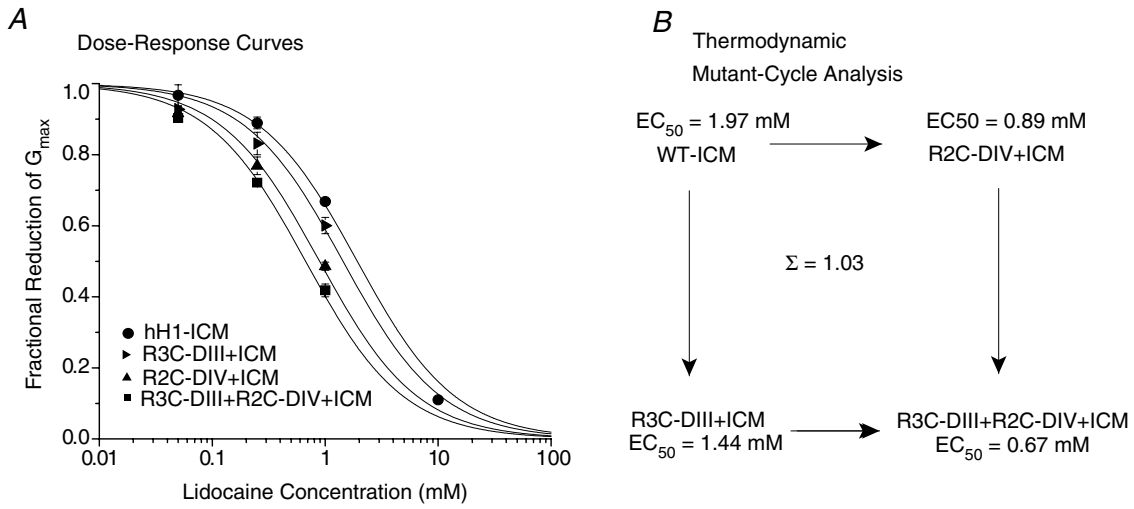

Figure 9. Dose dependence of lidocaine block of MTSEA-biotin stabilized S4 mutant Na^+ channels with a modified fast inactivation gate

A, single-site binding curves for each of the four Na^+ channels with a modified fast inactivation gate after exposure of the ICM mutation to intracellular MTSET. For each mutation and at each concentration, the means are from three to five cells except only one WT-ICM cell was exposed to 10 mM lidocaine. The lines represent the mean of the individual fits to cells by a single-site binding curve (eqn (4)). The IC_{50} values were; 1.97 ± 0.03 mM for WT-ICM ($n = 3$ cells); 1.44 ± 0.17 mM for R3C-DIII + ICM ($n = 3$ cells); 0.89 ± 0.07 mM for R2C-DIV + ICM ($n = 4$ cells) and 0.67 ± 0.03 mM for R3C-DIII + R2C-DIV + ICM ($n = 5$ cells). All IC_{50} values for each mutation were significantly different from one another. *B*, thermodynamic mutant-cycle analysis showing the effects of R3CDIII + ICM and R2CDIV + ICM on lidocaine block were additive (i.e. independent). Each corner of the of the cycle indicates the IC_{50} for the corresponding Na^+ channel mutation with WT-ICM in the upper left corner and R3C-DIII + R2C-DIV + ICM in the lower right hand corner. The coupling coefficient, Ω, was calculated using eqn (5). Note that as Ω approaches a value of 1 it indicates that the stabilization of one S4 segment acts independently of the other S4 segment.

be noted that pre-positioning both voltage sensors in the absence of fast inactivation reduced the IC_{50} to only 670 μM, a value more than an order of magnitude greater than the minimum achieved (28 μM) with intact inactivation. Consequently, it is reasonable to postulate that the pre-positioning of one or more of the S4s from domains III and IV achieved by MTSEA-biotin$_o$ in the absence of fast inactivation was not ideal. In support of this possibility we know that pre-positioning the voltage sensor in domain IV by MTSEA-biotin was consistent with a nearly completely outward, depolarized position (see Figs 3 and 4) while previous experiments have shown the S4-DIV in wild-type channels to be only partially inhibited by lidocaine (Sheets & Hanck, 2003). Another possibility is that the binding of the inactivation gate to its receptor exerts an additional, unknown but important effect on the lidocaine binding site, and the combination of the two S4s and the inactivation gate is required for the channel to assume its highest-affinity conformation.

However, it is clear that binding of the inactivation gate is not required for local anaesthetic drugs to alter the *Q–V* relationship, although much higher concentrations are required. The 35% gating charge reduction in WT-ICM$_{MTSETi}$ after intracellular perfusion with 20 mM QX-222, a quaternary amine analogue of lidocaine, was comparable to that found for native cardiac Na^+ channels (Hanck *et al.* 1994; Hanck *et al.* 2000). This finding is consistent with the previous study of Vedantham & Cannon (1999) who suggested that the drug-bound channel was not necessarily associated with a fast-inactivated state of the Na^+ channel because lidocaine did not protect the cysteine in the mutated ICM inactivation gate from modification by intracellular MTSET. Previously, they had shown that channels with the ICM mutation that had undergone fast inactivation were protected from modification by MTSET$_i$ (Vedantham & Cannon, 1998).

One mechanism that may explain, at least in part, the effect of fast inactivation on lidocaine block involves the interaction between the movement of the channel's voltage sensors and fast inactivation. In previous studies fast inactivation had been shown to slow (i.e. immobilize) the movement of nearly 60% of Na^+ channel gating charge during recovery from fast inactivation (Armstrong & Bezanilla, 1977; Sheets *et al.* 2000), resulting from the slow movement of the S4s in domains III and IV (Cha *et al.* 1999). However, after the specific disruption of the fast inactivation gate in WT-ICM by intracellular MTSET, the S4-DIII no longer became immobilized, and it recovered with rapid kinetics similar to the gating charge from domains I and II (Sheets *et al.* 2000; Sheets & Hanck, 2005). Consequently, the presence of fast inactivation may help to maintain the S4-DIII in an outward, depolarized position favouring lidocaine binding (Sheets & Hanck, 2003), while the removal of fast inactivation may facilitate the movement of the S4-DIII back to a rested, closed position. It may also be the case that voltage sensor position and/or lidocaine binding to the channel pore promotes channel conformations that have been identified as 'slow-inactivated'. No studies on the relationship of slow inactivation to voltage sensor positions of Na^+ channels are currently available, so such possibilities remain as speculation.

The lidocaine binding site and the S4 segments in domains III and IV

Significant progress has been made on determinating the most important residues that help form the local anaesthetic binding site within the inner vestibule of the Na^+ channel pore. Site-directed mutagenesis experiments investigating the local anaesthetic binding site determined that localized residues in the S6 segments of domains III and IV have the greatest influence on use-dependent drug block (Ragsdale *et al.* 1994; Li *et al.* 1999; Wang *et al.* 2000; Yarov-Yarovoy *et al.* 2001) while a single residue in S6-DI has also been identified (Nau *et al.* 1999; Yarov-Yarovoy *et al.* 2002). Mutations in the S6-DII appear to have no effect on drug block (Nau *et al.* 1999; Wang *et al.* 2001; Yarov-Yarovoy *et al.* 2002). Two hydrophobic residues, Phe-1759 and Tyr-1766 (using $Na_V1.5$ numbering) (Ragsdale *et al.* 1996), near the middle of the S6-DIV and two hydrophobic residues, Leu-1461 and to a lesser extent Ile-1465 (Yarov-Yarovoy *et al.* 2001) in the S6-DIII have been shown to affect lidocaine block. Phe-1759 makes the largest contribution and is widely held to be the most critical residue because its substitution by non-aromatic residues completely abolishes use-dependent block (McNulty *et al.* 2007). It should be mentioned that local anaesthetic drugs also exhibit a second type of block, a low affinity flicker-block (also referred to as fast block) that occurs at the selectivity filter (e.g. see Gingrich *et al.* 1993; Zamponi *et al.* 1993), which remains when fast inactivation is absent (Kimbrough & Gingrich, 2000).

It is widely believed that the molecular conformation of the Na^+ channel pore has similarities to the pores of the bacterial KcsA and MthK K^+ channels that have been determined crystallographically (Doyle *et al.* 1998; Jiang *et al.* 2002). The MthK crystal structure represents an open channel in which the inner helices of the four pore facing segments bend/rotate at a hinge point formed by a glycine residue to open the channel, while in the closed state (for KcsA) they form a bundle crossing (Jiang *et al.* 2002; MacKinnon, 2003). A similar conformation of an activation gate may occur in voltage-gated Na^+ channels because they also have conserved glycine residues in the first three S6 segments while the S6 in domain IV has a conserved serine (Goldin, 1995). Using the MthK channel

as a template, Lipkind and Fozzard modelled the pore and inner vestibule of the activated $Na_V1.4$ channel (Lipkind & Fozzard, 2005) and $Na_V1.5$ (McNulty *et al.* 2007) to permit energetically appropriate docking of local anaesthetic drugs in combination with the results of previously reported site-directed mutagenesis data. They found that in the most energetically favourable configuration for block of I_{Na}, the aromatic ring of lidocaine interacted with the Tyr in the S6-DIV while the alkylamino head docked with both the Phe in the S6-DIV and the Leu in the S6-DIII. Interestingly, these latter two residues in different S6 segments were separated by a narrow cavity (about 6 Å in width) that could dock the alkylamine head of lidocaine.

This leads to speculation about the relationship of Na^+ channel voltage sensors to the S6 segments and the activation gate. In the voltage-gated K^+ channel, $K_v1.2$, it is thought that the S4 segments pull on their corresponding S4–S5 linkers thus allowing the S6s to bend into an open position at glycine residues in the S6 segments during depolarization (Long *et al.* 2005). If the open state configuration of the Na^+ channel optimized the docking of the alkylamine head of lidocaine with both Phe in S6-DIV and Leu in S6-DIV, then lidocaine may in turn brace the S6s in an 'open' position thereby helping to stabilize their S4s in an outward, depolarized position. It is intriguing to suggest that the presence of a serine in S6-DIV, instead of a glycine that is present in the other three S6 segments, may be important if lidocaine were to 'brace' the S6-DIII in an open position. It should be noted that Na^+ channel opening can occur with little or no movement of the S4-DIV when the Na^+ channel is modified by site-3 toxins (Sheets & Hanck, 1995; Sheets *et al.* 1999; Chanda & Bezanilla, 2002). The model by Long *et al.* (2005) also places the voltage sensor domain in one K^+ channel subunit next to the pore domain in the adjacent subunit, consequently raising the possibility of coupling the voltage sensor domain in one subunit to the pore domain in another subunit (Soler-Llavina *et al.* 2006). Such a coupling effect may explain the finding that mutations at N434 (numbering based upon the rat skeletal muscle Na^+ channel) in the S6-DI affect channel kinetics and lidocaine affinity (Nau *et al.* 1999; Yarov-Yarovoy *et al.* 2002; McNulty *et al.* 2006). It remains uncertain as to whether or not such a possibility would have an effect on lidocaine binding when the S4s from the domains III and/or IV are pre-positioned in a Na^+ channel.

The Lipkind–Fozzard model also suggests a mechanism by which the S4 segments in domains III and IV may contribute to use-dependent block by lidocaine. During membrane depolarization, the S4 segments (in particular the S4-DIII) would be driven to an outward position thereby creating a crevice between the Leu in the S6-DIII and the Phe in the S6-DIV while simultaneously exposing the second docking site, Tyr one turn below Phe in S6-DIV. During repolarization, the S4-DIII would tend to return to a rested, closed position thereby eliminating the crevice that formed part of lidocaine's high affinity binding site. The presence of fast inactivation would help delay the tendency of the S4-DIII to move back to a rested, closed position thereby helping to maintain a configuration with a high affinity binding site, while the opposite would occur in the absence of fast inactivation. Our results on stabilization of the S4 in R3C-DIII + ICM support this model. Stabilization of the S4 in R2C-DIV + ICM also contributed to an increase in lidocaine affinity, and, in fact, its role may be greater than that of the S4-DIII as reflected by the smaller IC_{50} of R2C-DIV + ICM (890 μM) compared to that for R3C-DIII + ICM (1440 μM). Inspection of the Lipkind–Fozzard model places one of the two docking sites (the Phe) on the S6-DIV between the selectivity filter and the bundle crossing that may form the activation gate while the second docking site (Tyr) is placed at the bundle crossing. As a consequence, the second docking site may not be readily accessible until the channel opens even though the first docking may be accessible to a lipophilic molecule while the channel is in a closed position. Our results suggest that the two possible contact sites on domain IV make a somewhat greater contribution to lidocaine affinity than the docking site on domain III, although all three contact sites would allow for an even higher affinity binding. Lastly, it may be the combination of both the S4s in domains III and IV and the inactivation gate that permit the channel to assume its highest-affinity conformation for local anaesthetic drugs.

Of course the actual molecular details of the Na^+ channel are still unknown. Homology modelling of Na^+ channels with available crystal structures in combination with insights from site-directed mutagenesis drug studies and from experiments like those presented here should provide testable predictions of additional channel conformations that may contribute to therapeutically important interactions between local anaesthetic drugs and Na^+ channels. Despite the finding that lidocaine causes the S4-DIII in wild-type Na^+ channels to be completely stabilized in an outward, depolarized position (Sheets & Hanck, 2003), it may be the more modest effect of lidocaine on the movement of the S4-DIV that makes a greater contribution to the binding affinity of lidocaine, and thus underlies the use-dependent block central to these agents being effective antiarrhythmic drugs.

References

Armstrong CM & Bezanilla F (1977). Inactivation of the sodium channel. II. Gating current experiments. *J Gen Physiol* **70**, 567–590.

Balser JR, Nuss HB, Orias DW, Johns DC, Marban E, Tomaselli GF & Lawrence JH (1996). Local anesthetics as effectors of allosteric gating: Lidocaine effects on inactivation-deficient rat skeletal muscle Na channels. *J Clin Invest* **98**, 2874–2886.

Bennett PB, Valenzueka C, Chen L-Q & Kallen RG (1995). On the molecular nature of the lidocaine receptor of cardiac Na^+ channels. *Circulation Res* **77**, 584–592.

Cahalan MD (1978). Local anesthetic block of sodium channels in normal and pronase-treated squid giant axons. *Biophys J* **23**, 285–311.

Catterall WA (2000). From ionic currents to molecular mechanisms: the structure and function of voltage-gated sodium channels. *Neuron* **26**, 13–25.

Cha A, Ruben PC, George AL Jr, Fujimoto E & Bezanilla F (1999). Voltage sensors in domains III and IV, but not I and II, are immobilized by Na^+ channel fast inactivation. *Neuron* **22**, 73–87.

Chanda B & Bezanilla F (2002). Tracking voltage-dependent conformational changes in skeletal muscle sodium channel during activation. *J Gen Physiol* **120**, 629–645.

Chen Z, Ong BH, Kambouris NG, Marban E, Tomaselli GF & Balser JR (2000). Lidocaine induces a slow inactivated state in rat skeletal muscle sodium channels. *J Physiol* **524**, 37–49.

Chen LQ, Santarelli V, Horn R & Kallen RG (1996). A unique role for the S4 segment of domain 4 in the inactivation of sodium channels. *J Gen Physiol* **108**, 549–556.

Darman RB, Ivy AA, Ketty V & Blaustein RO (2006). Constraints on voltage sensor movement in the shaker K^+ channel. *J Gen Physiol* **128**, 687–699.

Doyle DA, Cabral JM, Pfuetzner RA, Kuo A, Gulbis JM, Cohen SL, Chait BT & MacKinnon R (1998). The structure of the potassium channel: molecular basis of K^+ conduction and selectivity. *Science* **280**, 69–77.

Gingrich KJ, Beardsley D & Yue DT (1993). Ultra-deep blockade of Na^+ channels by a quaternary ammonium ion: Catalysis by a transition-intermediate state? *J Physiol* **471**, 319–341.

Goldin AL (1995). Voltage-gated sodium channels. In *Handbook of Receptors and Channels: Ligand and Voltage-Gated Ion Channels*, ed. North RA, pp. 73–112. CRC Press, Boca Raton, FL, USA.

Greeff NG, Keynes RD & Van Helden DF (1982). Fractionation of the asymmetry current in the squid giant axon into inactivating and non-inactivating components. *Proc R Soc Lond B Biol Sci* **215**, 375–389.

Hanck DA, Makielski JC & Sheets MF (1994). Kinetic effects of quarternary lidocaine block of cardiac sodium channels: a gating current study. *J Gen Physiol* **103**, 19–43.

Hanck DA, Makielski JC & Sheets MF (2000). Lidocaine alters activation gating of cardiac Na channels. *Pflugers Arch* **439**, 814–821.

Hanck DA & Sheets MF (1992). Effects of extracellular divalent and trivalent cations on the kinetics of the sodium current in single canine cardiac Purkinje cells. *J Physiol* **454**, 267–298.

Hanck DA & Sheets MF (1995). Modification of inactivation in cardiac sodium channels: Ionic current studies with Anthopleurin-A toxin. *J Gen Physiol* **106**, 601–616.

Hanck DA & Sheets MF (2007). Site-3 toxins and cardiac sodium channels. *Toxicon* **49**, 181–193.

Hartmann HA, Tiedeman AA, Chen SF, Brown AM & Kirsch GE (1994). Effects of III–IV linker mutations on human heart Na^+ channel inactivation gating. *Circ Res* **75**, 114–122.

Hidalgo P & MacKinnon R (1995). Revealing the architecture of a K^+ channel pore through mutant cycles with a peptide inhibitor. *Science* **268**, 307–310.

Higuchi R, Krummel B & Saiki RK (1988). A general method of in vitro preparation and specific mutagenesis of DNA fragments: study of protein and DNA interactions. *Nucleic Acids Res* **16**, 7351–7367.

Hille B (1977). Local anesthetics: Hydrophilic and hydrophobic pathways for the drug-receptor reaction. *J Gen Physiol* **69**, 497–515.

Ho SN, Hunt HD, Horton RM, Pullen JK & Pease LR (1989). Site-directed mutagenesis by overlap extension using the polymerase chain reaction [see comments]. *Gene* **77**, 51–59.

Hondeghem LM & Katzung BG (1977). Time- and voltage-dependent interaction of antiarrhythmic drugs with cardiac sodium channels. *Biochim Biophys Acta* **472**, 373–398.

Horovitz A & Fersht AR (1990). Strategy for analysing the co-operativity of intramolecular interactions in peptides and proteins. *J Mol Biol* **214**, 613–617.

Jiang Y, Lee A, Chen J, Cadene M, Chait BT & MacKinnon R (2002). The open pore conformation of potassium channels. *Nature* **417**, 523–526.

Jiang Y, Ruta V, Chen J, Lee A & MacKinnon R (2003). The principle of gating charge movement in a voltage-dependent K^+ channel. *Nature* **423**, 42–48.

Kimbrough JT & Gingrich KJ (2000). Quaternary ammonium block of mutant Na^+ channels lacking inactivation: features of a transition-intermediate mechanism. *J Physiol* **529**, 93–106.

Li HL, Galue A, Meadows L & Ragsdale DS (1999). A molecular basis for the different local anesthetic affinities of resting versus open and inactivated states of the sodium channel. *Mol Pharmacol* **55**, 134–141.

Lipkind GM & Fozzard HA (2005). Molecular modeling of local anesthetic drug binding by voltage-gated sodium channels. *Mol Pharmacol* **68**, 1611–1622.

Long SB, Campbell EB & Mackinnon R (2005). Voltage sensor of Kv1.2: structural basis of electromechanical coupling. *Science* **309**, 903–908.

MacKinnon R (2003). Potassium channels. *FEBS Lett* **555**, 62–65.

Makielski JC, Ye B, Valdivia CR, Pagel MD, Pu J, Tester DJ & Ackerman MJ (2003). A ubiquitous splice variant and a common polymorphism affect heterologous expression of recombinant human SCN5A heart sodium channels. *Circ Res* **93**, 821–828.

McNulty MM, Edgerton GB, Shah RD, Hanck DA, Fozzard HA & Lipkind GM (2007). Charge at the lidocaine binding site residue Phe-1759 affects permeation in human cardiac voltage-gated sodium channels. *J Physiol* **581**, 741–755.

McNulty MM, Kyle JW, Lipkind GM & Hanck DA (2006). An inner pore residue (Asn406) in the Nav1.5 channel controls slow inactivation and enhances mibefradil block to T-type Ca^{2+} channel levels. *Mol Pharmacol* **70**, 1514–1523.

Meves H & Vogel W (1977). Inactivation of the asymmetrical displacement current in giant axons of *Loligo forbesi*. *J Physiol* **267**, 377–393.

Nau C & Wang GK (2004). Interactions of local anesthetics with voltage-gated Na^+ channels. *J Membr Biol* **201**, 1–8.

Nau C, Wang SY, Strichartz GR & Wang GK (1999). Point mutations at N434 in D1–S6 of mu1 Na^+ channels modulate binding affinity and stereoselectivity of local anesthetic enantiomers. *Mol Pharmacol* **56**, 404–413.

Nonner W (1980). Relations between the inactivation of sodium channels and the immobilization of gating charge in frog myelinated nerve. *J Physiol* **299**, 573–603.

Provencher SW (1976). A Fourier method for the analysis of exponential decay curves. *Biophys J* **16**, 27–41.

Qiu XQ, Jakes KS, Finkelstein A & Slatin SL (1994). Site-specific biotinylation of colicin Ia. A probe for protein conformation in the membrane. *J Biol Chem* **269**, 7483–7488.

Ragsdale DS, McPhee JC, Scheuer T & Catterall WA (1994). Molecular determinants of state-dependent block of Na^+ channels by local anesthetics. *Science* **265**, 1724–1728.

Ragsdale DS, McPhee JC, Scheuer T & Catterall WA (1996). Common molecular determinants of local anesthetic, antiarrhythmic, and anticonvulsant block of voltage-gated Na^+ channels. *Proc Natl Acad Sci U S A* **93**, 9270–9275.

Sheets MF & Hanck DA (1995). Voltage-dependent open-state inactivation of cardiac sodium channels: Gating currents studies with Anthopleurin-A toxin. *J Gen Physiol* **106**, 617–640.

Sheets MF & Hanck DA (2002). The outermost lysine in the S4 of domain III contributes little to the gating charge in sodium channels. *Biophys J* **82**, 3048–3055.

Sheets MF & Hanck DA (2003). Molecular action of lidocaine on the voltage sensors of sodium channels. *J Gen Physiol* **121**, 163–175.

Sheets MF & Hanck DA (2005). Charge immobilization of the voltage sensor in domain IV is independent of sodium current inactivation. *J Physiol* **563**, 83–93.

Sheets MF, Kyle JW & Hanck DA (2000). The role of the putative inactivation lid in sodium channel gating current immobilization. *J Gen Physiol* **115**, 609–620.

Sheets MF, Kyle JW, Kallen RG & Hanck DA (1999). The Na channel voltage sensor associated with inactivation is localized to the external charged residues of domain IV, S4. *Biophys J* **77**, 747–757.

Sheets MF, Kyle JW, Krueger S & Hanck DA (1996). Optimization of a mammalian expression system for the measurement of sodium channel gating currents. *Am J Physiol Cell Physiol* **271**, C1001–C1006.

Slatin SL, Qiu XQ, Jakes KS & Finkelstein A (1994). Identification of a translocated protein segment in a voltage-dependent channel. *Nature* **371**, 158–161.

Soler-Llavina GJ, Chang TH & Swartz KJ (2006). Functional interactions at the interface between voltage-sensing and pore domains in the Shaker K_v channel. *Neuron* **52**, 623–634.

Starkus JG, Fellmeth BD & Raynor MD (1981). Gating currents in the intact crayfish giant axon. *Biophys J* **35**, 521–533.

Strichartz GR (1973). The inhibition of sodium currents in myelinated nerve by quaternary derivitives of lidocaine. *J Gen Physiol* **62**, 37–57.

Takahashi MP & Cannon SC (2001). Mexiletine block of disease-associated mutations in S6 segments of the human skeletal muscle Na^+ channel. *J Physiol* **537**, 701–714.

Vedantham V & Cannon SC (1998). Slow inactivation does not affect movement of the fast inactivation gate in voltage-gated Na^+ channels. *J Gen Physiol* **111**, 83–93.

Vedantham V & Cannon SC (1999). The position of the fast-inactivation gate during lidocaine block of voltage-gated Na^+ channels. *J Gen Physiol* **113**, 7–16.

Wang SY, Barile M & Wang GK (2001). Disparate role of Na^+ channel D2–S6 residues in batrachotoxin and local anesthetic action. *Mol Pharmacol* **59**, 1100–1107.

Wang SY, Nau C & Wang GK (2000). Residues in Na^+ channel D3–S6 segment modulate both batrachotoxin and local anesthetic affinities. *Biophys J* **79**, 1379–1387.

Yang NB, George AL Jr & Horn R (1996). Molecular basis of charge movement in voltage-gated sodium channels. *Neuron* **16**, 113–122.

Yang N & Horn R (1995). Evidence for voltage-dependent S4 movement in sodium channels. *Neuron* **15**, 213–218.

Yarov-Yarovoy V, Brown J, Sharp EM, Clare JJ, Scheuer T & Catterall WA (2001). Molecular determinants of voltage-dependent gating and binding of pore-blocking drugs in transmembrane segment IIIS6 of the Na^+ channel α subunit. *J Biol Chem* **276**, 20–27.

Yarov-Yarovoy V, McPhee JC, Idsvoog D, Pate C, Scheuer T & Catterall WA (2002). Role of amino acid residues in transmembrane segments IS6 and IIS6 of the Na^+ channel α subunit in voltage-dependent gating and drug block. *J Biol Chem* **277**, 35393–35401.

Zamponi GW, Doyle DD & French RJ (1993). Fast lidocaine block of cardiac and skeletal muscle sodium channels: One site with two routes of access. *Biophys J* **65**, 80–90.

Acknowledgements

We thank WenQing Yu for her excellent technical assistance. This work was supported by NIH Grant HL-R01-44630 (MFS/DAH).